2005

Determination of Ion Exchange Parameters by a Genetic Algorithm

Brian R. West
Wilfrid Laurier University, bwest@wlu.ca

Seppo Honkanen
University of Arizona

Determination of ion exchange parameters by a genetic algorithm

Brian R. West
Seppo Honkanen
The University of Arizona
Optical Sciences Center
Tucson, Arizona 85721
E-mail: bwest@optics.arizona.edu

Abstract. Modeling the process of ion exchange in glass requires accurate knowledge of the self-diffusion coefficients of the incoming and outgoing ions. Furthermore, correlating the concentration profile of the incoming ions to a change in refractive index requires knowledge of the correlation coefficient. We present a method by which these three parameters can be quickly determined experimentally, using a genetic algorithm. Comparison with published data is presented. © *2005 Society of Photo-Optical Instrumentation Engineers.* [DOI: 10.1117/1.2048752]

Subject terms: ion exchange; waveguide; diffusion coefficients; refractive index; genetic algorithm; numerical optimization.

Paper 040917R received Dec. 1, 2004; revised manuscript received Feb. 23, 2005; accepted for publication Mar. 9, 2005; published online Sep. 15, 2005.

1 Introduction

Ion exchange in a glass substrate is a proven method for producing optical waveguides. The relative ease by which low-loss waveguides can be fabricated with low birefringence and excellent mode-matching to single-mode fiber makes ion exchange a promising alternative to competing technologies such as chemical vapor deposition and sol-gel coating.[1] Long used for the production of passive telecommunication devices, ion exchange has recently found applications in active devices[2] and sensing.[3]

The ion exchange process is described by the binary diffusion equation[4]:

$$\frac{\partial C_A}{\partial t} = \frac{D_A}{1-(1-M)C_A}\left[\nabla^2 C_A + \frac{(1-M)(\nabla C_A)^2}{1-(1-M)C_A} - \frac{q\mathbf{E}_{\text{ext}}}{kT}\nabla C_A\right], \quad (1)$$

where D_A is the self-diffusion coefficient of the incoming ionic species in the substrate glass; and $M=D_A/D_B$, where D_B is the self-diffusion coefficient of the outgoing ionic species, and C_A is the concentration of the incoming ions, normalized with respect to the saturated concentration. The saturated concentration is dependent on the stoichiometry of the substrate and melt, and as such, its exact value is usually unknown. Instead, it is common to normalize C_A to equal unity at the surface of the substrate that is in contact with the salt, and zero far away from this interface. Here $\mathbf{E}_{\text{ext}}$ is the applied electric field, while T, k, and q are the absolute temperature, Boltzmann's constant, and the electron charge, respectively. In all practical cases, solution of Eq. (1) requires numerical methods, as discussed in Ref. 5.

For small absolute concentrations of incoming ions, the change in refractive index over that of the substrate is proportional to the ion concentration:

$$n(x,y,\lambda) = n_{\text{sub}}(\lambda) + \Delta n_0(\lambda) C_A(x,y), \quad (2)$$

where n_{sub} is the substrate index; and Δn_0 is the constant of proportionality, which is equal to the largest index change. The latter parameter is determined empirically, which justifies the use of the normalized concentration C_A.

To accurately determine the index profile using Eqs. (1) and (2), it is critical that the diffusion parameters D_A and M, and the proportionality constant Δn_0, are precisely known. None of these values are routinely provided by the substrate manufacturers; they must be determined experimentally. This procedure generally consists of the following steps: (1) processing of a slab (1-D) waveguide with no applied electric field; (2) measurement of the resulting index profile, or more frequently, measurement of the effective indices of the guided modes, with subsequent reconstruction of the index profile; and (3) determination of the parameters that produced this index profile. Early efforts to this end generally assumed a functional form for the index distribution,[6] allowing D_A and Δn_0 to be calculated quickly using the Wentzel-Kramer-Brillouin (WKB) dispersion relation. However, assuming a particular functional form of the refractive index is equivalent to specifying M. As the index profile can resemble a complementary error function (for $M=1$), parabola ($M\approx 0.5$), Gaussian profile ($M\approx 0.1$), or steplike profile ($M\ll 0.1$),[1] it is inadvisable to make such an assumption when there is no *a priori* information on the ion exchange system in question.

Simultaneous determination of D_A, M, and Δn_0 by comparison of measured and modeled effective mode indices was attempted by previous authors using what amounts to "brute force" methods.[7] In this procedure, the diffusion equation (1) is solved numerically for assumed values of D_A and M, and the resulting concentration profile is converted to an index profile for an assumed value of Δn_0. The effective mode indices are solved for, and compared in a squared-error sense with those measured from the fabricated waveguide using a prism coupler. The parameters are

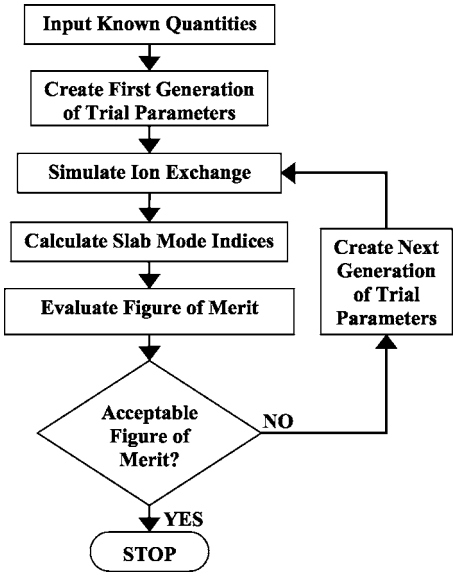

Fig. 1 Flowchart illustrating the GA used for ion exchange parameter extraction.

altered until the squared error is acceptably minimized. Given the nonlinearity of Eq. (1), this can be a very labor-intensive process.

In this paper, we describe a novel method of determining the ion exchange parameters that utilizes a genetic algorithm. This technique provides accurate results with a minimum of effort on behalf of the operator. Section 2 describes the algorithm. In Sec. 3, we use the algorithm to determine parameters of a particular glass, and compare them with those found in Ref. 7. The implications of this method for more complex ion exchange systems are discussed briefly in Sec. 4.

2 Description of the Genetic Algorithm for Parameter Extraction

The genetic algorithm (GA), generally attributed to De Jong,[8] is a conceptual reduction of Darwin's theory of natural selection.[9] The solution of a physical problem is optimized by treating trial solutions as the individuals within a population of "organisms," which must evolve to conform to the conditions set forth by the problem at hand. By selecting the best individuals of a generation and combining their characteristics, individuals from subsequent generations will *on average* approach the optimum solution to the problem. Unlike traditional derivative-based optimization algorithms, the GA is not prone to becoming trapped in local extrema of the fitness function in "optimization space" (the set of all possible combinations of the parameters to be optimized). Rather, the application of random mutations enables the GA to escape such extrema to optimize solutions globally. In addition, derivative-based methods require that the function to be optimized is "smooth" (i.e., continuous and differentiable everywhere), a restriction that does not apply to GAs.

The GA is particularly well-suited to "inverse" problems—those for which an outcome is known and modeling of the forward process is feasible, but for which several initial conditions or physical parameters must be determined. The problem of ion exchange parameter extraction falls into this category. The GA for parameter extraction is described in the flowchart shown in Fig. 1, with each step described in the following.

Table 1 Example of 8-bit binary representation of parameter M, where M varies from 0.1 to 0.61.

M	Gene
0.100	00000000
0.102	00000001
0.104	00000010
⋮	⋮
0.608	11111110
0.610	11111111

2.1 *Input Known Quantities and Create a First Generation of Trial Parameters*

The operator must input the known values of the prism coupling wavelength, the substrate index at this wavelength (which is easily observed as the "knee" of the prism coupling spectrum), the measured slab mode indices $n_{\mathrm{eff},m}$, and the ion exchange time. Upper and lower bounds for all three parameters must be provided as well. A narrow region of parameter space will accelerate convergence to a solution, so any *a priori* knowledge is of great benefit. One such constraint is that the lower limit of Δn_0 must be at least $n_{\mathrm{eff},1}-n_{\mathrm{sub}}$. A final input is the resolution with which each parameter must be known.

Each parameter is binary-encoded into a bit string, commonly referred to as a "gene," with the least significant bit representing the specified resolution of the parameter. An example is shown in Table 1. The three genes are then concatenated into a "chromosome," as illustrated in Fig. 2. The initial population of trial parameter sets is randomly generated using a uniform distribution (each bit is equally likely to be "0" or "1").

2.2 *Simulate Ion Exchange and Calculate Slab Mode Indices*

In one dimension and with no applied electric field, Eq. (1) becomes

$$\frac{\partial C_A}{\partial t}=\frac{D_A}{1-(1-M)C_A}\left[\frac{\partial^2 C_A}{\partial y}+\frac{(1-M)(\partial C_A/\partial y)^2}{1-(1-M)C_A}\right]. \tag{3}$$

With only one spatial dimension of interest, both explicit and implicit methods can be employed to rapidly solve Eq.

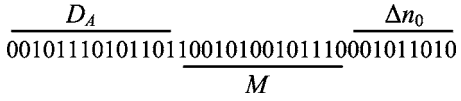

Fig. 2 Illustration of the concatenation of genes into a chromosome that uniquely identifies a trial set of parameters.

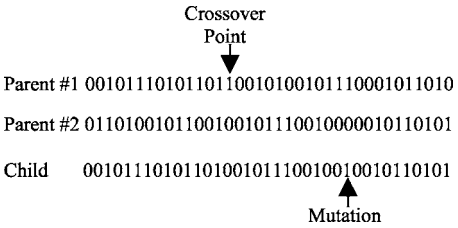

Fig. 3 Combination of genetic information by single-point crossover and mutation.

(3), with stability issues managed by employing suitably small time steps and grid spacing. This GA employs the implicit three-point Crank-Nicolson method[10] to solve for $C_A(y,t)$. The Dirichlet conditions $C_A(0,t)=1$ and $C_A(h,t)=0$ are used, where h is the deepest point in the computational domain.

The index profile is calculated from the concentration profile using Eq. (2) and the trial value of Δn_0. Effective indices $N_{\text{eff},m}$ of all guided slab modes are calculated using a fast algorithm derived from the WKB equation.[11]

2.3 *Evaluate Figure of Merit*

Each trial set of parameters is evaluated by comparing the resulting set of mode indices to those measured by the prism coupler, and assigning a "figure of merit" F to the parameters:

$$F = \exp\left\{-\left[\sum_m w_m (N_{\text{eff},m} - n_{\text{eff},m})^2\right]\right\}. \quad (4)$$

A weighted sum of squared errors is used here. The errors are squared as in Ref. 7 to ensure that F is reduced for errors in index of either sign. The weights w_m are optional elements in F that reflect the differing levels of confidence in the measured modes. Those that lie just above cutoff are generally less accurate due to their proximity to the substrate "knee" in the prism coupling spectrum. The exponential drop-off in F for large mode errors serves to bias the following generation toward an optimal solution, as described in the following subsection.

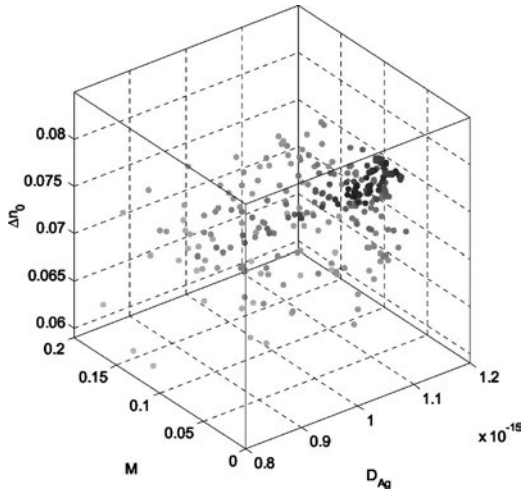

Fig. 4 Results of the genetic algorithm for extraction of ion exchange parameters. Each dot represents a trial solution evaluated within the algorithm. The fitness is represented by shade—lighter dots represent very poor fitness, while darker dots represent very good fitness.

Table 2 Input data and results of the GA.

Parameter	Symbol	Value
Exchange time	t_{ex}	30 min
Exchange temperature	T	324°C
Wavelength	λ	632.8 nm
Substrate index	n_{sub}	1.5210
Measured effective indices	$n_{\text{eff},m}$	1.5870, 1.5702, 1.5565, 1.5433, 1.5311
Weights	w_m	5, 4, 3, 2, 1
Generations	N_G	20
Simulations per generation	S_G	15
Self-diffusion coefficient of Ag^+	D_{Ag}	1.09×10^{-15} m^2/s
Ratio of self-diffusion coefficients	M	0.074
Maximum index change	Δn_0	0.075

2.4 *Create the Next Generation of Trial Parameters*

If none of the trial sets of parameters produces an acceptably high figure of merit, it is necessary to create a new generation of chromosomes. To accomplish this, "parent" chromosomes are selected in proportion to their figure of merit—a process known as "roulette wheel scaling"[12]—and their genetic material is combined using a single-point crossover. A small probability of mutation of a random bit is allowed. This is illustrated in Fig. 3.

3 Application of the GA

The GA described in the previous section was used to determine the temperature-dependent ion exchange parameters for a Schott IOG-10 substrate undergoing silver-sodium exchange in a 10% $AgNO_3$ melt. To enable a direct comparison with the results of Ref. 7, identical effective index data are used for slab waveguides fabricated at a variety of temperatures and over a range of exchange times. Figure 4 illustrates the output of the GA for one particular set of input data, which is shown in Table 2. Each dot within the figure represents a trial set of parameters; the shade of the dot represents its figure of merit. Note that the

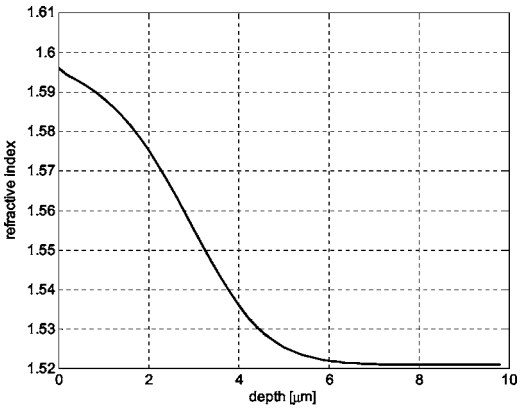

Fig. 5 Comparison of refractive index profile reconstructed from measured modes (dotted line) and modeled from results of genetic algorithm (solid line).

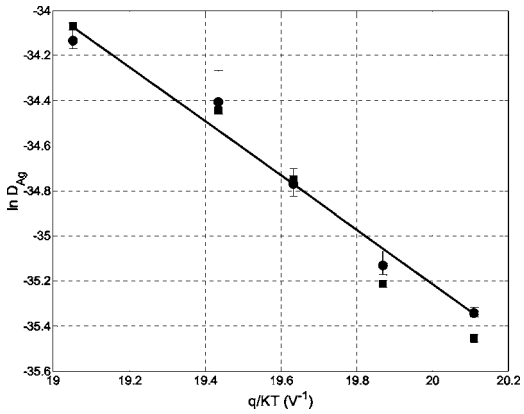

Fig. 6 Graph of ln (D_{Ag}) versus (q/kT). Results of the GA are shown as circles, with error bars indicating the range of values for different exchange times. The solid line represents a linear fit to the GA results. Results of Ref. 7 are shown as squares.

self-diffusion coefficient D_A is now denoted D_{Ag}, indicating that silver is the incoming ion. Figure 5 compares the refractive index profile arising from the results of the GA with that reconstructed from the measured modes.[13] The profiles are virtually indistinguishable.

Note that the self-diffusion coefficients are strongly temperature-dependent. As ionic mobility depends on a microscopic level on the probability that an ion's kinetic energy exceeds the activation energy required to break free from its site in the glass matrix, D_{Ag} exhibits Arrhenius behavior[1]:

$$D_{Ag}(T) = D_{Ag0} \exp\left(\frac{-E_a}{kT}\right), \tag{5}$$

where E_a is the activation energy. Plotting ln (D_{Ag}) versus ($1/kT$) should produce a straight line of slope $-E_a$. Any data that deviate considerably from this line are erroneous, suggesting that the GA be allowed to evolve further (or possibly that the bounds on parameter values are incorrect). In addition to improving the accuracy of the parameters, knowledge of the temperature dependence enables the parameter values to be extrapolated to the lower temperatures commonly encountered in field-assisted or annealing processes. At these temperatures, D_{Ag} may be sufficiently low that fabricating a slab waveguide by thermal exchange from a salt melt would take a prohibitive length of time. In fact, it may be impossible if the temperature of interest falls below the salt's melting temperature.

Figure 6 shows the results of the GA over a range of temperatures. The natural logarithm of D_{Ag} is plotted against (q/kT), where the vertical error bars indicate the range of calculated diffusion coefficients for different exchange times. The data show a strong linear trend, as expected (regression coefficient $r^2=0.9734$). The circles represent the values of D_{Ag} calculated in Ref. 7. The value of M was found to equal 0.074 for all temperatures (averaged over exchange time). While M is expected to vary with temperature, this dependence is considerably weaker than that of D_{Ag}, and is not appreciable over the narrow temperature range used. While the authors of Ref. 7 claim a significant linear trend in the Stewart coefficient α (equal to $1-M$), the data in their Table 1 does not clearly show this over the small temperature range. For example, their calculated α values do not decrease monotonically with temperature, as expected. In all cases, the calculated value of Δn_0 was 0.075.

4 Discussion

The ion exchange model of Eq. (1) used in this simulation describes the exchange of two species of mobile ions. While this is sufficient in most common substrates in current use, the need may arise for modeling of ternary (or higher order) ion exchange, for substrates that contain two or more species of network modifiers with substantial concentration and mobility. In this case, Eq. (1) is no longer strictly true. Fortunately, this issue is avoided through the combined efforts of parameter extraction and process modeling. As the parameter extraction algorithm uses experimentally obtained effective index data as input, the calculated parameters can be thought of as "effective" physical constants, which may have been perturbed by any number of additional physical effects. These same parameters are subsequently used in the process modeling, which also utilizes Eq. (1) (see, for example, Ref. 5), making the full modeling process self-consistent from an engineering standpoint.

Acknowledgments

The authors would like to thank James Carriere and Jesse Frantz for fabricating and characterizing the slab waveguides used in this study. In addition, the authors acknowledge the support from Technology Research Incentive Funding (TRIF).

References

1. S. I. Najafi, *Introduction to Glass Integrated Optics*, Artech House, Norwood, MA (1992).
2. D. L. Veasey, D. S. Funk, P. M. Peters, N. A. Sanford, G. E. Obarski, N. Fontaine, M. Young, A. P. Peskin, W.-C. Liu, S. N. Houde-Walter, and J. S. Hayden, "Yb/Er-codoped and Yb-doped waveguide lasers in phosphate glass," *J. Non-Cryst. Solids* **263**(1–4), 369–381 (2000).
3. C. R. Lavers, K. Itoh, S. C. Wu, M. Murabayashi, I. Mauchline, G. Stewart, and T. Stout, "Planar optical waveguides for sensing applications," *Sens. Actuators B* **69**(1), 85–95 (2000).
4. J. Albert, and J. W. Y. Lit, "Full modeling of field-assisted ion exchange for graded index buried channel optical waveguides," *Appl. Opt.* **29**(18), 2798–2804 (1990).
5. B. R. West, P. Madasamy, N. Peyghambarian, and S. Honkanen, "Modeling of ion-exchanged glass waveguide structures," *J. Non-Cryst. Solids* **347**(1–3), 18–26 (2004).
6. G. L. Yip and J. Albert, "Characterization of planar optical waveguides by K^+-ion exchange in glass," *Opt. Lett.* **10**(3), 151–153 (1985).
7. P. Y. Choo, J. A. Frantz, J. T. A. Carriere, D. L. Mathine, R. K. Kostuk, and N. Peyghambarian, "Measurement and modeling of ion-exchange parameters for IOG-10 glass," *Opt. Eng.* **42**(10), 2812–2816 (2003).
8. K. De Jong, "An analysis of the behaviour of a class of genetic adaptive systems," PhD Dissertation, University of Michigan (1975).
9. C. Darwin, *On the Origin of Species*, John Murray, London (1859).
10. C. F. Gerald and P. O. Wheatley, *Applied Numerical Analysis*, 5th ed., Addison-Wesley, Reading, MA (1994).
11. K. S. Chiang, "Effective-index function method for the analysis and design of inhomogeneous planar waveguides based on the WKB equation," *Opt. Commun.* **84**(5–6), 258–263 (1991).
12. L. Davis, *Handbook of Genetic Algorithms*, Van Nostrand Reinhold, New York (1991).
13. K. S. Chiang, "Construction of refractive-index profiles of planar dielectric waveguides from the distribution of effective indexes," *J. Lightwave Technol.* **3**(2), 385–391 (1985).

Brian R. West received his BEng degree in engineering physics from McMaster University in 1997, his MS degree in engineering sciences from the Thayer School of Engineering, Dartmouth College, in 1999, and his MS and PhD degrees in optical sciences in 2002 and 2004, respectively, from the Optical Sciences Center, University of Arizona. Previously, Dr. West was a research scientist with MPB Communications, working in the area of fiber-based devices.

Seppo Honkanen is an associate professor of optical sciences with the University of Arizona. He attended Helsinki University of Technology and received his MS and PhD degrees in electrical engineering in 1984 and 1988, respectively. He has been with the University of Arizona since 1995, but while on leave from 1999 to 2001, he was a vice president of business development and vice president of research and development at NP Photonics. Previously, Dr. Honkanen was a principal scientist of optoelectronics and a manager of integrated optics with Nokia Research Center. He is a coauthor of over 70 scientific publications in peer-reviewed journals.